

Dual-comb self-mode-locked monolithic Yb:KGW laser with orthogonal polarizations

M. T. Chang,¹ H. C. Liang,² K. W. Su,¹ and Y. F. Chen^{1,3,*}

¹ Department of Electrophysics, National Chiao Tung University, 1001 Ta-Hsueh Rd. Hsinchu 30010, Taiwan

² Institute of Optoelectronic Science, National Taiwan Ocean University, Keelung 20224, Taiwan

³ Department of Electronics Engineering, National Chiao Tung University, Hsinchu 30010, Taiwan
yfchen@cc.nctu.edu.tw

Abstract: The dependence of lasing threshold on the output transmission is numerically analyzed to find the condition for the gain-to-loss balance for the orthogonal N_p and N_m polarizations with a N_g -cut Yb:KGW laser crystal. With the numerical analysis, an orthogonally polarized dual-comb self-mode-locked operation is experimentally achieved with a coated Yb:KGW crystal to form a monolithic cavity. At a pump power of 5.2 W, the average output power, the pulse repetition rate, and the pulse duration are measured to be 0.24 (0.6) W, 25.8 (25.3) GHz, and 1.06 (1.12) ps for the output along the N_p (N_m) polarization.

©2015 Optical Society of America

OCIS codes: (140.3480) Lasers, diode-pumped; (140.3580) Lasers, solid-state; (140.3615) Lasers, ytterbium.

References and links

1. B. Wu, P. Jiang, D. Yang, T. Chen, J. Kong, and Y. Shen, "Compact dual-wavelength Nd:GdVO₄ laser working at 1063 and 1065 nm," *Opt. Express* **17**(8), 6004–6009 (2009).
2. A. A. Sirotkin, S. V. Garnov, V. I. Vlasov, A. I. Zagumennyi, Y. D. Zavartsev, S. A. Kutovoi, and I. A. Shcherbakov, "Two-frequency vanadate lasers with mutually parallel and orthogonal polarizations of radiation," *Quantum Electron.* **42**(5), 420–426 (2012).
3. A. Brenier, Y. Wu, P. Fu, J. Zhang, and Y. Zu, "Diode-pumped laser properties of Nd³⁺-doped La₂CaB₁₀O₁₉ crystal including two-frequency generation with 4.6 THz separation," *Opt. Express* **17**(21), 18730–18737 (2009).
4. Y. P. Huang, C. Y. Cho, Y. J. Huang, and Y. F. Chen, "Orthogonally polarized dual-wavelength Nd:LuVO₄ laser at 1086 nm and 1089 nm," *Opt. Express* **20**(5), 5644–5651 (2012).
5. Y. J. Chen, X. H. Gong, Y. F. Lin, J. H. Huang, Z. D. Luo, and Y. D. Huang, "Diode-pumped orthogonally polarized dual-wavelength Nd³⁺:LaBO₂MoO₄ laser," *Appl. Phys. B* **112**(1), 55–60 (2013).
6. Y. Zhao, S. Zhuang, X. Xu, J. Xu, H. Yu, Z. Wang, and X. Xu, "Anisotropy of laser emission in monoclinic, disordered crystal Nd:LYSO," *Opt. Express* **22**(3), 2228–2235 (2014).
7. J. Min, B. Yao, P. Gao, R. Guo, B. Ma, J. Zheng, M. Lei, S. Yan, D. Dan, T. Duan, Y. Yang, and T. Ye, "Dual-wavelength slightly off-axis digital holographic microscopy," *Appl. Opt.* **51**(2), 191–196 (2012).
8. S. N. Son, J. J. Song, J. U. Kang, and C. S. Kim, "Simultaneous second harmonic generation of multiple wavelength laser outputs for medical sensing," *Sensors (Basel)* **11**(12), 6125–6130 (2011).
9. S. L. Zhang, Y. D. Tan, and Y. Li, "Orthogonally polarized dual frequency lasers and applications in self-sensing metrology," *Meas. Sci. Technol.* **21**(5), 054016 (2010).
10. A. Schliesser, M. Brehm, F. Keilmann, and D. van der Weide, "Frequency-comb infrared spectrometer for rapid, remote chemical sensing," *Opt. Express* **13**(22), 9029–9038 (2005).
11. I. Coddington, W. C. Swann, and N. R. Newbury, "Coherent multiheterodyne spectroscopy using stabilized optical frequency combs," *Phys. Rev. Lett.* **100**(1), 013902 (2008).
12. B. Bernhardt, A. Ozawa, P. Jaquet, M. Jacquy, Y. Kobayashi, T. Udem, R. Holzwarth, G. Guelachvili, T. Hänsch, and N. Piqué, "Cavity-enhanced dual-comb spectroscopy," *Nat. Photonics* **4**(1), 55–57 (2010).
13. A. Bartels, R. Cerna, C. Kistner, A. Thoma, F. Hudert, C. Janke, and T. Dekorsy, "Ultrafast time-domain spectroscopy based on high-speed asynchronous optical sampling," *Rev. Sci. Instrum.* **78**(3), 035107 (2007).
14. Y. F. Chen, W. Z. Zhuang, H. C. Liang, G. W. Huang, and K. W. Su, "High-power subpicosecond harmonically mode-locked Yb:YAG laser with pulse repetition rate up to 240 GHz," *Laser Phys. Lett.* **10**(1), 1–4 (2012).
15. G. Q. Xie, D. Y. Tang, L. M. Zhao, L. J. Qian, and K. Ueda, "High-power self-mode-locked Yb:Y₂O₃ ceramic laser," *Opt. Lett.* **32**(18), 2741–2743 (2007).
16. A. Lagatsky, C. Brown, and W. Sibbett, "Highly efficient and low threshold diode-pumped Kerr-lens mode-locked Yb:KYW laser," *Opt. Express* **12**(17), 3928–3933 (2004).
17. W. Z. Zhuang, M. T. Chang, H. C. Liang, and Y. F. Chen, "High-power high-repetition-rate subpicosecond monolithic Yb:KGW laser with self-mode locking," *Opt. Lett.* **38**(14), 2596–2599 (2013).
18. A. Brenier, "Active Q-switching of the diode-pumped two-frequency Yb³⁺:KGd(WO₄)₂ laser," *IEEE J. Quantum Electron.* **47**(3), 279–284 (2011).

19. F. Krausz, T. Brabec, and C. Spielmann, "Self-starting passive mode locking," *Opt. Lett.* **16**(4), 235–237 (1991).
20. M. Zhou, D. X. Cao, M. Z. Wang, X. F. Wang, and Y. M. Luo, "Polarized fluorescence spectra analysis of Yb³⁺:KGd(WO₄)₂," *Opt. Commun.* **282**(20), 4109–4113 (2009).
21. J. Dong, A. Shirakawa, K. I. Ueda, and A. A. Kaminskii, "Effect of ytterbium concentration on cw Yb:YAG microchip laser performance at ambient temperature - Part II: Theoretical modeling," *Appl. Phys. B* **89**(2–3), 367–376 (2007).
22. T. Taira, W. M. Tulloch, and R. L. Byer, "Modeling of quasi-three-level lasers and operation of cw Yb:YAG lasers," *Appl. Opt.* **36**(9), 1867–1874 (1997).
23. V. E. Kisel, A. E. Troshin, V. G. Shcherbitsky, and N. V. Kuleshov, "Luminescence lifetime measurements in Yb³⁺-doped KY(WO₄)₂ and KGd(WO₄)₂," in *Advanced Solid-State Photonics*, OSA Technical Digest (Optical Society of America, 2004), paper WB7.
24. W. D. Tan, D. Y. Tang, C. W. Xu, J. Zhang, H. H. Yu, and H. J. Zhang, "Dual-wavelength passively mode-locked Nd:GdVO₄ laser with orthogonal polarizations," *Appl. Phys. B* **102**(4), 775–779 (2011).

1. Introduction

Various Nd-doped gain media have been widely employed to generate dual-wavelength laser sources [1–6] for the applications on laser interferometry, precision measurement, medical instrumentation, holographic microscopy, and differential absorption lidar [7–9]. In recent years, dual-comb mode-locked lasers with slightly different pulse repetition rates have also started to attract much attention due to the applications on laser spectroscopy [10–12] and asynchronous optical sampling for pump-probe measurements without mechanical delay [13].

Comparing with Nd-doped laser crystals, Yb-doped gain media have been confirmed to be superior materials for generating efficient ultrashort mode-locked lasers due to the small quantum defect, broad absorption and fluorescence spectra, and elimination of parasitic effects. Recently, the diode-pumping scheme has been successfully used to achieve efficient self-mode-locked operations in Yb-doped crystal lasers [14–16]. Here, the meaning of the self-mode locking (SML) is that no additional active or passive mode-locking elements (such as saturable absorbers) are used in the laser cavity except for the gain medium. So far, the origin of the SML is conjectured to come from the combined effects of the Kerr-lensing and thermal lensing together with gain aperture [14,15]. More recently, a self-mode-locked laser with a repetition rate up to 22.4 GHz has been successfully demonstrated by using a coated Yb:KGW crystal to form a monolithic cavity [17]. With the large emission band of the Yb:KGW crystal, it is highly desirable to develop an orthogonally polarized dual-wavelength Yb:KGW laser with the SML operation. Even though the Yb:KGW crystal has been utilized to achieve an orthogonally polarized dual-wavelength Q-switched operation [18], the development for the dual-comb SML laser has not been demonstrated thus far.

Here we report on the use of a coated N_g -cut Yb:KGW crystal as a monolithic cavity to achieve the orthogonally polarized dual-comb SML operation. We numerically analyze the dependence of the lasing thresholds on the output transmission T for the orthogonal N_p and N_m polarizations to find that the gain-to-loss balance for the orthogonal polarizations can be feasible with a value of T near 1~2%. Based on the numerical analysis, we design a coated Yb:KGW crystal to obtain the orthogonally polarized dual-comb SML operation. At a pump power of 5.2 W, the average output powers along N_p and N_m polarizations are 0.6 W and 0.24 W, respectively. The pulse repetition rate is 25.8 GHz and 25.3 GHz for the laser output along the N_p and N_m polarization, respectively. The pulse duration is 1.06 ps and 1.12 ps for the N_p and N_m polarization

2. Numerical analysis

The Kerr-lens mode locking that employs the Kerr nonlinearity of the gain medium itself and the soft aperture formed by the pumped volume in the gain medium has been identified to be an extremely simple means of ultrafast optical modulation [19]. A simple formulism derived by Krausz *et al.* to analyze the self-starting threshold of the passive mode locking from mode beating fluctuations in a free-running solid-state laser is given by [19]

$$(\kappa P_i)_{th} > \frac{1}{\ln(m)} \frac{T_r}{T_c} \quad (1)$$

where κ is a characteristic of the Kerr nonlinearity used for passive mode locking, P_i is the circulating average intracavity power in the free running laser, T_r is the cavity round-trip time, and T_c is effective correlation time between the longitudinal modes in the free-running laser. Equation (1) reveals that a decrease in T_r can significantly reduce the intensity needed for self-starting at a fixed κ . We experimentally found that combing the high Kerr nonlinearity of the KGW crystal with the high-Q monolithic short cavity can directly achieve the continuous wave SML without the phenomenon of Q-switched mode locking.

Next, polarization dependent absorption and emission spectra were measured with an optical spectrum analyzer with a resolution of 0.5 nm. The gain medium was a Yb:KGW crystal with Yb³⁺ doping concentration of 5 at.% and its length was approximately 3 mm. The Yb:KGW crystal shows anisotropic properties along its three orthogonal refractive index axes which are labeled as N_m , N_p , and N_g , resulting in polarization dependent absorption and emission spectra. The present Yb:KGW crystal was cut along the N_g -axis to obtain the higher absorption and emission cross sections along the N_m or N_p principal axes. The measured data were calibrated by comparing with the results in ref [20]. Figures 1(a) and 1(b) depict the experimental results for the absorption and emission cross sections, respectively. The absorption and emission cross sections along the N_m axis are obviously larger than those along the N_p axis for the wavelength in the range of 970–1030 nm. On the other hand, the absorption and emission spectra reveal that the Yb:KGW crystal has the capacity for simultaneously dual-comb emission with orthogonal polarizations for the wavelength near 1050 nm.

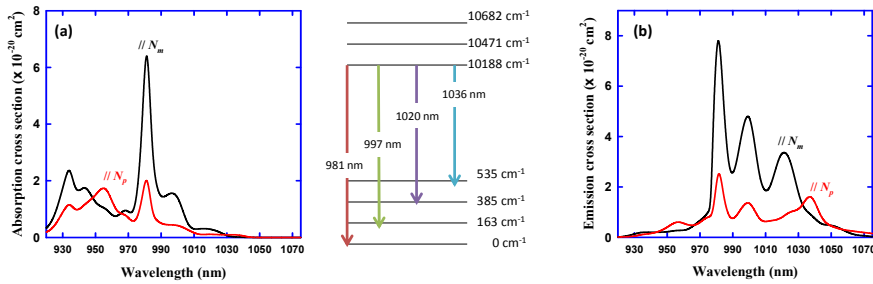


Fig. 1. Experimental results for the (a) absorption and (b) emission cross sections of the N_g -cut Yb:KGW crystal along the N_m and N_p principal axes. The inset is the energy levels.

Without polarization controlling elements, the emission wavelength of material is mainly determined by the gain-to-loss ratio which is governed by the pump condition, re-absorption loss, and useful output coupling [21]. Considering the absorption effect, the laser threshold power can be estimated from the equation [22]:

$$P_{th} = \frac{\pi h\nu_p (\omega_p^2 + \omega_c^2)}{4 \tau(\sigma_a + \sigma_e)(f_1 + f_2)} \left[T + L + 2(1 - e^{-\sigma_a N_1 l_c}) \right] \quad (2)$$

where ω_p and ω_c are the pump and cavity mode radii, $h\nu_p$ is the pump photon energy, τ is the emission life time, σ_a and σ_e are the absorption and emission cross sections at the laser wavelength, respectively, f_1 and f_2 are the fractional population in the upper and lower energy levels, T is the output coupling of the output coupler, L stands for the double-pass passive loss, N_1 is the population of the lower laser level at threshold, and l_c represents the length of the laser crystal. With the absorption and emission cross sections shown in Fig. 1(a) and (b) and using the parameter values of $\omega_p = 0.2$ mm and $\omega_c = 0.2$ mm, $\tau = 250$ μ s [23], $f_1 = 0.75$ and $f_2 = 0.04$, $N_1 = 1.7 \times 10^{20}$ cm^{-3} for the lower level at 385 cm^{-1} , $N_1 = 0.8 \times 10^{20}$ cm^{-3} for the lower level at 535 cm^{-1} , $L = 0.5\%$, the threshold pump power given by Eq. (1) was calculated as a function of the wavelength. Note that the value of L was estimated from the experimental data. Figures 2(a) and 2(b) show the calculated results for the output couplers of

$T = 5\%$ and $T = 1.5\%$, respectively. For the case of $T = 5\%$ shown in Fig. 2(a), the minimum lasing threshold can be seen to be near the wavelength of 1035 nm with the polarization along the N_m axis. For the case of $T = 1.5\%$ shown in Fig. 2(b), it can be seen that the N_m and N_p polarized states almost possess the same minimum lasing threshold near the wavelength of 1048 nm. In other words, the dual-comb laser emission with two orthogonal polarizations is possible to be obtained with an output coupler of T around 1.5%. In the following, we demonstrated an orthogonally polarized dual-comb monolithic Yb:KGW laser to confirm this analysis.

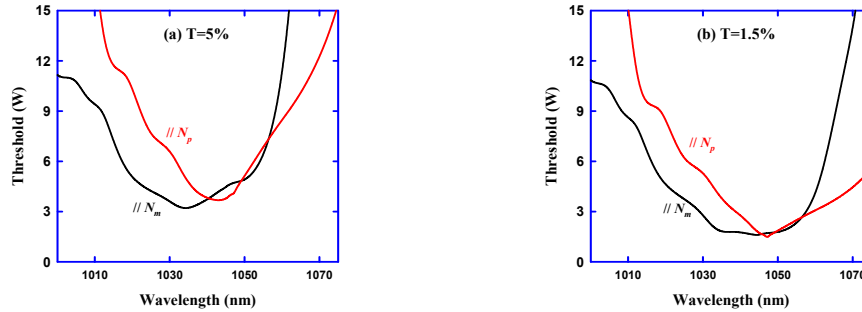


Fig. 2. Calculated results for the dependence of the threshold pump power on the laser wavelength of the Yb:KGW crystal for output coupling of (a) $T = 5\%$ and (b) $T = 1.5\%$.

3. Experimental results and discussion

Figure 3(a) depicts the scheme of exploiting a coated Yb:KGW crystal as a monolithic cavity. One of the end facet of the laser crystal was coated for high reflection (HR, $R > 99.8\%$) centered at 1065 nm with total spectral bandwidth of 70 nm (1030-1100 nm) and high transmission (HT, $T > 95\%$) at 980 nm to serve as a front mirror. The rear facet was coated for high reflection (HR, $R > 99\%$) at 980 nm to increase the absorption efficiency of the pump power and was coated for partial reflection (PR, $R \approx 98.5\%$) centered at 1050 nm with total spectral bandwidth of 40 nm (1030-1070 nm) to serve as an output coupler. Note that the output coupling T of the cavity was designed to be 1.5% as discussed above to achieve dual-comb operation. The Yb:KGW crystal was wrapped with indium foil and mounted within a water-cooled copper heat sink maintained at 8°C to ensure stable laser output. The pumping source was a 980 nm fiber-coupled laser diode with a core diameter of 200 μm and a numerical aperture of 0.2. A lens with a focal length of 25 mm was used to focus the pump beam into the laser crystal. The overall coupling efficiency was nearly 90%.

Figure 3(b) shows experimental results for the average output power of the dual-comb Yb:KGW laser with orthogonal polarizations versus the incident pump power. The total output power is found to reach 0.82 W under the pump power of 5.2 W, corresponding to a slope efficiency of 28.3% and an optical-to-optical efficiency of 16.0%. Experimental results revealed that both transverse modes of two orthogonally polarized states are the near TEM_{00} mode with the beam quality better than 1.3 for the pump power less than 5.2 W. It can be seen that the lasing with polarization along the N_p axis is prior to the lasing along the N_m axis. The threshold pump power is found to be 2.2 W for polarization parallel to the N_p axis and 2.5 W for N_m direction, rather consistent with the calculated result shown in Fig. 2(b). The output power with polarization along the N_p axis initially increases linearly with the pump power, and tends to get saturated at 0.24 W with the pump power higher than 3.9 W. On the other hand, the output power with polarization parallel to the N_m axis rises as the pump power increases with higher slope efficiency in comparison with the lasing along the N_p axis, up to 0.58 W at a pump power of 5.2 W. The outputs for two orthogonal polarizations have an equal power of 0.24 W at a pump power of 4.3 W. It is worthwhile to mention that the N_m polarized state turns out to be the high order mode for the pump power greater than 5.2 W.

Nevertheless, it is confirmed that the dual-comb laser operation displays good temporal stability without power competition between the two polarization states for the pump power less than 5.2 W.

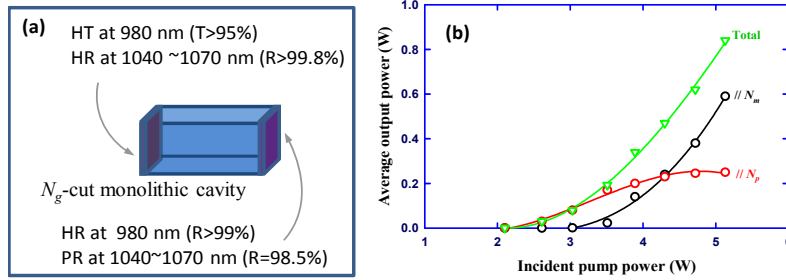


Fig. 3. (a) Schematic of the experimental cavity setup for the dual-comb self-mode-locked monolithic Yb:KGW laser. (b) Dependence of the average output power on the incident pump power with different polarizations.

The optical spectrum of the laser output was measured with a Michelson optical interferometer (Advantest, Q8347) with a resolution of 0.003 nm that is able to perform first-order autocorrelations by Fourier transforming the optical spectrum. Figure 4 depicts the experimental result for the lasing spectrum at the pump power of 4.3 W where the two polarization states have the same output power. It can be seen that there are dual lasing bands with central wavelengths at 1047.32 nm (N_p axis) and 1048.48 nm (N_m axis). The values of the full width at half maximum (FWHM) of the spectral bands at 1047.32 nm (N_p axis) and 1048.48 nm (N_m axis) are 1.6 nm and 1.5 nm, respectively. The longitudinal mode spacings within each spectral band are found to be 25.8 GHz (1047.32 nm, N_p axis) and 25.3 GHz (1048.48 nm, N_m axis). This mode spacing exactly corresponds to the free spectral range of the Yb:KGW crystal.

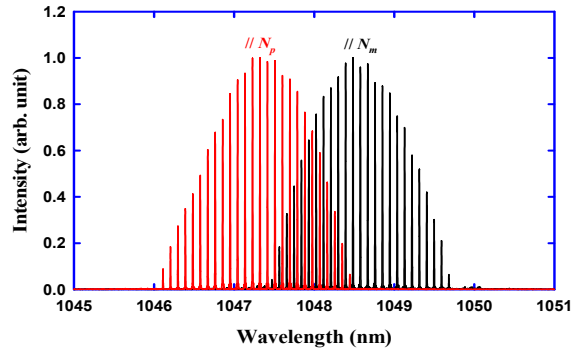


Fig. 4. Experimental optical spectrum of the dual-comb orthogonally polarized Yb:KGW laser.

The temporal behavior of the laser output was analyzed by exploiting the schemes of first- and second-order autocorrelations. The second-order autocorrelation trace was performed with a commercial autocorrelator (APE GmbH, PulseCheck). Figure 5 shows experimental results for the first-order autocorrelation trace at the pump power of 4.3 W. The pulse repetition rates are consistent with the mode spacings shown in Fig. 4. With the group indexes of 1.986 for the N_p axis and 2.023 for the N_m axis, the precise length of the Yb:KGW crystal was deduced to be 2.93 mm. Figures 6(a) and 6(b) show the FWHM widths of the single pulses in the second-order autocorrelation traces for two orthogonal polarizations. Assuming the Gaussian-shaped temporal profile, the pulse durations were estimated to be 1.06 ps for the N_p axis and 1.12 ps for the N_m axis. As a result, the time-bandwidth products of the SML

pulses were evaluated to be 0.463 and 0.458 for the N_p and N_m axes, respectively; both values are slightly greater than the Fourier-limited value of 0.441. The chirped pulses for two orthogonal polarizations mainly come from the group velocity dispersion induced by the gain medium. In comparison with other dual-band mode-locked laser with orthogonal polarization by utilizing the Nd:GdVO₄ crystal [24] which the output pulse duration is 7 ps, the significant reduction of the pulse duration shows the advantage of the Yb-doped materials with wider emission bandwidths.

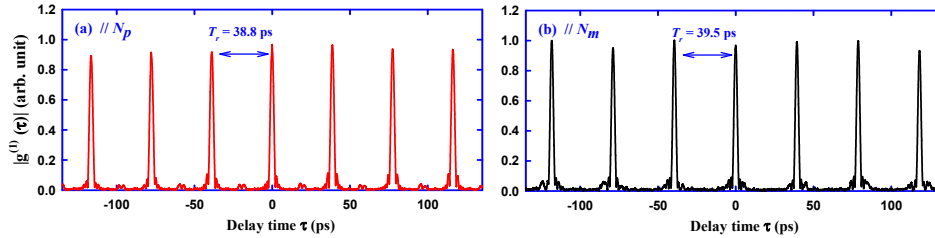


Fig. 5. Experimental traces of the temporal behavior of first-order autocorrelation for polarization direction along (a) N_p axis and (b) N_m axis.

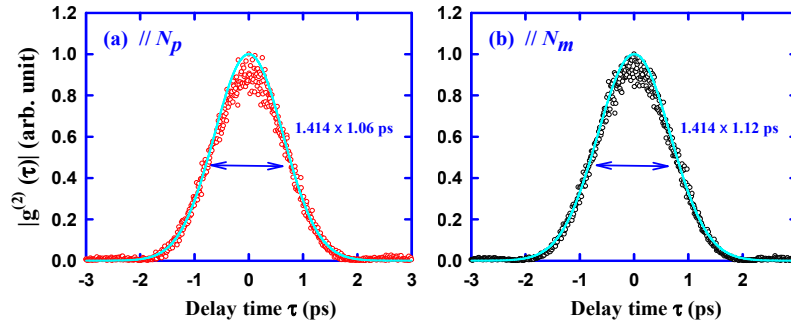


Fig. 6. FWHM width of a single pulse of the second-order autocorrelations for polarization direction along (a) N_p axis and (b) N_m axis.

4. Conclusion

In conclusion, we have analyzed the condition of gain-to-loss balance via tuning the output coupling in a Yb:KGW laser to achieve the orthogonally polarized dual-wavelength operation. Based on the numerical analysis, we have designed a monolithic Yb:KGW crystal laser to generate an orthogonally polarized dual-comb SML laser. At a pump power of 5.2 W, the average output powers along N_p and N_m polarizations are 0.6 W and 0.24 W, respectively. The pulse repetition rate and the pulse duration are found to be 25.8 (25.3) GHz and 1.06 (1.12) ps for the laser output along the N_p (N_m) polarization. We believe that the orthogonally polarized dual-comb monolithic SML laser is a promising light source for many applications.

Acknowledgments

The authors thank the National Science Council for the financial support of this research under Contract No. MOST 103-2112-M-009-0016-MY3.